

Scattering of a Plane Wave by a Small Conducting Sphere

Kirk T. McDonald

Joseph Henry Laboratories, Princeton University, Princeton, NJ 08544

(July 13, 2004; updated April 28, 2014)

1 Problem

Discuss the scattering of a plane electromagnetic wave of angular frequency ω that is incident on a perfectly conducting sphere of radius a , which is at rest, when the wavelength obeys $\lambda \gg a$ ($ka \ll 1$). Calculate the electromagnetic fields and the Poynting vector everywhere, and interpret these fields in both the near and far zones. Consider incident electromagnetic waves of both linear and circular polarization.

2 Solution

We review this well-known problem¹ with an emphasis on details of the fields close to the sphere (sec. 2.2), following the usual, briefer analysis that applies to the far zone (sec. 2.1).

A possible interest in a study of the near zone in this problem is its relation to the near-zone behavior of broadcast antennas. Although, the latter are not typically considered as examples of scattering phenomena, in a sense they are. An antenna is fed from an rf generator by a feedline that is often a coaxial cable. This cable carries power in the form of a TEM electromagnetic wave, that is delivered to the feedpoints of the antenna. One view of what follows is that the TEM wave scatters off the feedpoints of the antenna (as in Young's view of waves diffracted by an aperture), and the bulk structure of the antenna serves only to constrain or guide the scattered wave.

In the usual excellent approximation that the antenna is made of a perfect conductor, the tangential component of the total electric field must vanish everywhere on the antenna (in a frame where the antenna is at rest). Hence, the total Poynting vector [2], $\mathbf{S} = (c/4\pi)\mathbf{E} \times \mathbf{B}$ (in Gaussian units), cannot have a component that is perpendicular to any surface of the antenna. Thus, a discussion of energy flow of either an antenna or of scattering by a conducting sphere that is based on the total Poynting vector will consider these two problems to be similar.

A more "microscopic" view may be preferable to many people. The incident wave, be it a free-space plane wave or a TEM wave in a cable, excites time-dependent charge and current distributions in the sphere or antenna. Near- and far-zone fields, which include scattering (or radiation) terms, can then be deduced from a knowledge of the current distribution. The Poynting vector of these fields will include a component that is perpendicular to the surface of the sphere or antenna, which is sometimes interpreted as describing the local strength of the radiation emitted by a point on the sphere or antenna. This view follows from the spirit

¹The earliest study of this problem may be by J.J. Thomson in secs. 369-378 of [1].

of Poynting, but is somewhat at odds with the view of Huygens [3] in which wave phenomena are described by sum (interference) of contributions from distributed sources.

In the present problem it is relatively straightforward to deduce the current distribution in the conducting sphere for first principles. This is not generally the case in antenna problems, where one often proceeds from a plausible “guess” as to the form of the current distribution. As will be seen below, the total current distribution is proportional to, but not equal to, that part of the current distribution that can be said to drive to far-zone scattered (or radiation) fields.

2.1 Far-Zone Analysis: Scattering

The scattering cross section in spherical coordinates (r, θ, ϕ) is given by

$$\frac{d\sigma}{d\Omega} = \frac{\text{power scattered into } d\Omega}{\text{incident power per unit area}} = r^2 \frac{\langle \mathbf{S}_{\text{scat}}(\theta, \phi) \rangle}{\langle \mathbf{S}_{\text{incident}} \rangle} = r^2 \frac{|\mathbf{E}_{\text{scat}}|^2}{E_0^2}, \quad (1)$$

where in the dipole approximation, the far-zone scattered electric field is [4, 5, 6]

$$\mathbf{E}_{\text{scat}} = k^2 \frac{e^{i(kr-\omega t)}}{r} [(\hat{\mathbf{n}} \times \mathbf{p}_0) \times \hat{\mathbf{n}} - \hat{\mathbf{n}} \times \mathbf{m}_0], \quad (2)$$

and $\mathbf{p}_0 e^{i\omega t}$ and $\mathbf{m}_0 e^{-i\omega t}$ are the electric and magnetic dipole moments induced in the conducting sphere by the incident wave.

Because the incident wavelength is large compared to the radius of the sphere, the incident fields are essentially uniform over the sphere, and the induced fields near the sphere are the same as the static fields of a conducting sphere in an otherwise uniform electric and magnetic field. Then, from p. 57 of the Notes,² the induced electric dipole moment is given by

$$\mathbf{p}_0 = a^3 \mathbf{E}_0. \quad (3)$$

For the induced magnetic dipole, we recall p. 98 of the Notes,³ remembering that a conducting sphere can be thought of a permeable sphere with zero permeability and a dielectric sphere of infinite dielectric constant. Hence, the magnetic dipole moment is

$$\mathbf{m}_0 = -\frac{a^3}{2} \mathbf{B}_0. \quad (4)$$

Then,

$$\mathbf{E}_{\text{scat}} = -k^2 a^3 \frac{e^{i(kr-\omega t)}}{r} \left[\hat{\mathbf{n}} \times (\mathbf{E}_0 \times \hat{\mathbf{n}}) + \frac{1}{2} (\hat{\mathbf{n}} \times \mathbf{B}_0) \right], \quad (5)$$

where $\hat{\mathbf{n}}$ is along the vector \mathbf{r} that points from the center of the sphere to the distant observer.

For a wave propagating in the $+z$ direction with electric field linearly polarized along direction $\hat{\mathbf{l}}$, $\mathbf{E}_0 = E_0 \hat{\mathbf{l}}$, and the magnetic field obeys $\mathbf{B}_0 = \hat{\mathbf{z}} \times \mathbf{E}_0$. Then,

$$\begin{aligned} \mathbf{E}_{\text{scat}} &= -k^2 a^3 E_0 \frac{e^{i(kr-\omega t)}}{r} \left[\hat{\mathbf{n}} \times (\hat{\mathbf{l}} \times \hat{\mathbf{n}}) + \frac{1}{2} \hat{\mathbf{n}} \times (\hat{\mathbf{z}} \times \hat{\mathbf{l}}) \right] \\ &= -k^2 a^3 E_0 \frac{e^{i(kr-\omega t)}}{r} \left[\hat{\mathbf{l}} \left(1 - \frac{(\hat{\mathbf{n}} \cdot \hat{\mathbf{z}})}{2} \right) - \left(\hat{\mathbf{n}} - \frac{\hat{\mathbf{z}}}{2} \right) (\hat{\mathbf{n}} \cdot \hat{\mathbf{l}}) \right]. \end{aligned} \quad (6)$$

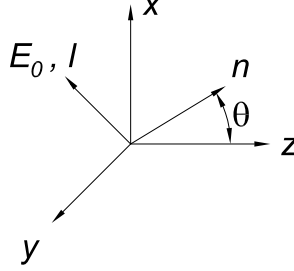
²<http://physics.princeton.edu/~mcdonald/examples/ph501/ph501lecture5.pdf>

³<http://physics.princeton.edu/~mcdonald/examples/ph501/ph501lecture8.pdf>

Inserting this in (1) we find

$$\frac{d\sigma}{d\Omega} = k^4 a^6 \left[\left(1 - \frac{\hat{\mathbf{n}} \cdot \hat{\mathbf{z}}}{2} \right)^2 - \frac{3}{4} (\hat{\mathbf{n}} \cdot \hat{\mathbf{1}})^2 \right]. \quad (7)$$

For an observer in the x - z plane, $\hat{\mathbf{n}} \cdot \hat{\mathbf{z}} = \cos \theta$. Then, for electric polarization parallel to the scattering plane $\hat{\mathbf{n}} \cdot \hat{\mathbf{1}} = \sin \theta$, while for polarization perpendicular to the scattering plane $\hat{\mathbf{n}} \cdot \hat{\mathbf{1}} = 0$.



Thus, eq. (7) yields

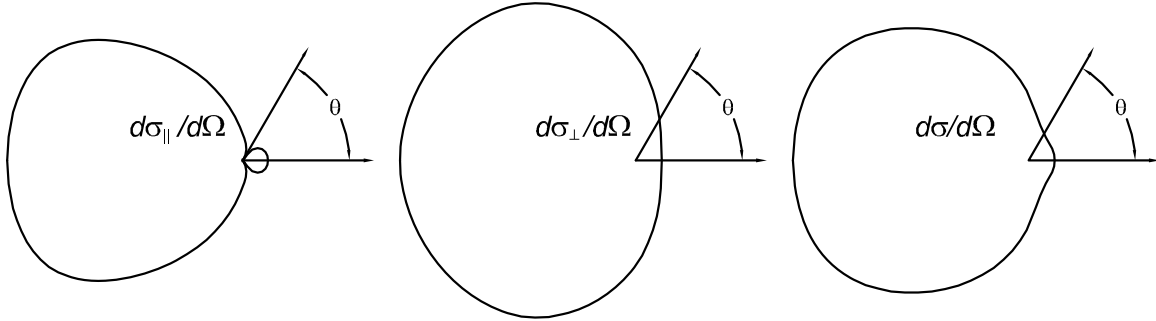
$$\frac{d\sigma_{\parallel}}{d\Omega} = k^4 a^6 \left(\frac{1}{2} - \cos \theta \right)^2, \quad \frac{d\sigma_{\perp}}{d\Omega} = a^6 k^4 \left(1 - \frac{\cos \theta}{2} \right)^2. \quad (8)$$

For an unpolarized incident wave,

$$\frac{d\sigma}{d\Omega} = \frac{1}{2} \left(\frac{d\sigma_{\parallel}}{d\Omega} + \frac{d\sigma_{\perp}}{d\Omega} \right) = k^4 a^6 \left[\frac{5}{8} (1 + \cos^2 \theta) - \cos \theta \right], \quad (9)$$

and so⁴

$$\sigma = \int \frac{d\sigma}{d\Omega} d\Omega = \frac{10\pi}{8} k^4 a^6 \int_{-1}^1 (1 + \cos^2 \theta) d \cos \theta = \frac{10\pi a^2}{3} k^4 a^4. \quad (10)$$



⁴The cross section (10) varies as $1/\lambda^4$ in contrast to the Thomson scattering cross section for a free electron [7], $\sigma_{\text{Thomson}} = 8\pi r_e^2/3$, where $r_e = e^2/m_e c^2$ is the classical electron radius, which is independent of wavelength (for $\lambda \ll \lambda_{\text{Compton}} = h/m_e c$). While the conduction electrons in a metallic object of characteristic length a are “free,” they are not free to leave the object, and are bound to it by a force that can be approximated as springlike with a characteristic angular frequency $\omega_0 \approx c/a$. Then, scattering of electromagnetic waves with angular frequency $\omega = kc \ll \omega_0 \approx c/a$, *i.e.*, for $ka \ll 1$, varies as $\omega^4/\omega_0^4 \propto 1/\lambda^4$, as discussed, for example, on pp. 278-279 of the Notes,

<http://physics.princeton.edu/~mcdonald/examples/ph501/ph501lecture23.pdf>

A consequence is that the total scattering cross section is smaller than the geometric cross section $\approx \pi a^2$ by a factor of order $(ka)^4 \ll 1$. These general conclusions are verified for small metallic spheres via Maxwell’s equations in the present example. And, this behavior holds for scattering by small metallic disks [8, 9, 10], for which $\sigma \approx 128\pi a^2 (ka)^4 / 27\pi^2$.

From eqs. (8) we see that $d\sigma_{\perp}/d\Omega$ is always nonzero, but $d\sigma_{\parallel}/d\Omega = 0$ for $\theta = \pi/3$, so for this angle, the scattered radiation is linearly polarized parallel to the scattering plane for arbitrary incident polarization.

2.2 Near-Zone Analysis

To discuss the fields in the near zone, we can use the full forms of fields from Hertzian dipoles [4, 5, 6]. Thus, the scattered electric field at any position \mathbf{r} outside the sphere is

$$\begin{aligned}\mathbf{E}_{\text{scat}}(\mathbf{r}, t) &= k^2 \frac{e^{i(kr-\omega t)}}{r} \left\{ (\hat{\mathbf{n}} \times \mathbf{p}_0) \times \hat{\mathbf{n}} + [3(\hat{\mathbf{n}} \cdot \mathbf{p}_0)\hat{\mathbf{n}} - \mathbf{p}_0] \left(\frac{1}{k^2 r^2} - \frac{i}{kr} \right) \right. \\ &\quad \left. - \left(1 + \frac{i}{kr} \right) \hat{\mathbf{n}} \times \mathbf{m}_0 \right\} \\ &= k^2 a^3 \frac{e^{i(kr-\omega t)}}{r} \left\{ (\hat{\mathbf{n}} \times \mathbf{E}_0) \times \hat{\mathbf{n}} + [3(\hat{\mathbf{n}} \cdot \mathbf{E}_0)\hat{\mathbf{n}} - \mathbf{E}_0] \left(\frac{1}{k^2 r^2} - \frac{i}{kr} \right) \right. \\ &\quad \left. + \frac{1}{2} \left(1 + \frac{i}{kr} \right) \hat{\mathbf{n}} \times \mathbf{B}_0 \right\},\end{aligned}\tag{11}$$

also using eqs. (3) and (4). From now on we suppose that the electric field of the incident plane wave is along the x -axis, so that $\mathbf{E}_0 = E_0 \hat{\mathbf{x}}$ and $\mathbf{B}_0 = E_0 \hat{\mathbf{y}}$, while the point of observation is at $\mathbf{r} = (r, \theta, \phi)$. We express the electric field vector in spherical coordinates, noting that

$$\hat{\mathbf{n}} = \hat{\mathbf{r}},\tag{12}$$

$$\hat{\mathbf{x}} = \sin \theta \cos \phi \hat{\mathbf{r}} + \cos \theta \cos \phi \hat{\boldsymbol{\theta}} - \sin \phi \hat{\boldsymbol{\phi}},\tag{13}$$

$$\hat{\mathbf{y}} = \sin \theta \sin \phi \hat{\mathbf{r}} + \cos \theta \sin \phi \hat{\boldsymbol{\theta}} + \cos \phi \hat{\boldsymbol{\phi}},\tag{14}$$

$$\hat{\mathbf{z}} = \cos \theta \hat{\mathbf{r}} - \sin \theta \hat{\boldsymbol{\theta}}.\tag{15}$$

Thus,

$$\begin{aligned}\mathbf{E}_{\text{scat}}(\mathbf{r}, t) &= k^2 a^3 E_0 \frac{e^{i(kr-\omega t)}}{r} \left\{ \cos \theta \cos \phi \hat{\boldsymbol{\theta}} - \sin \phi \hat{\boldsymbol{\phi}} \right. \\ &\quad \left. + (2 \sin \theta \cos \phi \hat{\mathbf{r}} - \cos \theta \cos \phi \hat{\boldsymbol{\theta}} + \sin \phi \hat{\boldsymbol{\phi}}) \left(\frac{1}{k^2 r^2} - \frac{i}{kr} \right) \right. \\ &\quad \left. - \frac{1}{2} \left(1 + \frac{i}{kr} \right) (\cos \phi \hat{\boldsymbol{\theta}} - \cos \theta \sin \phi \hat{\boldsymbol{\phi}}) \right\} \\ &= k^2 a^3 E_0 \frac{e^{i(kr-\omega t)}}{r} \left\{ 2 \sin \theta \cos \phi \left(\frac{1}{k^2 r^2} - \frac{i}{kr} \right) \hat{\mathbf{r}} \right. \\ &\quad \left. + \cos \phi \left[\cos \theta \left(1 - \frac{1}{k^2 r^2} + \frac{i}{kr} \right) - \frac{1}{2} \left(1 + \frac{i}{kr} \right) \right] \hat{\boldsymbol{\theta}} \right. \\ &\quad \left. - \sin \phi \left[1 - \frac{1}{k^2 r^2} + \frac{i}{kr} - \frac{\cos \theta}{2} \left(1 + \frac{i}{kr} \right) \right] \hat{\boldsymbol{\phi}} \right\}.\end{aligned}\tag{16}$$

Similarly, the scattered magnetic field can be written

$$\begin{aligned}
\mathbf{B}_{\text{scat}}(\mathbf{r}, t) &= k^2 \frac{e^{i(kr-\omega t)}}{r} \left\{ (\hat{\mathbf{n}} \times \mathbf{m}_0) \times \hat{\mathbf{n}} + [3(\hat{\mathbf{n}} \cdot \mathbf{m}_0)\hat{\mathbf{n}} - \mathbf{m}_0] \left(\frac{1}{k^2 r^2} - \frac{i}{kr} \right) \right. \\
&\quad \left. + \left(1 + \frac{i}{kr} \right) \hat{\mathbf{n}} \times \mathbf{p}_0 \right\} \\
&= -k^2 a^3 \frac{e^{i(kr-\omega t)}}{2r} \left\{ (\hat{\mathbf{n}} \times \mathbf{B}_0) \times \hat{\mathbf{n}} + [3(\hat{\mathbf{n}} \cdot \mathbf{B}_0)\hat{\mathbf{n}} - \mathbf{B}_0] \left(\frac{1}{k^2 r^2} - \frac{i}{kr} \right) \right. \\
&\quad \left. - 2 \left(1 + \frac{i}{kr} \right) \hat{\mathbf{n}} \times \mathbf{E}_0 \right\} \\
&= -k^2 a^3 E_0 \frac{e^{i(kr-\omega t)}}{2r} \left\{ \cos \theta \sin \phi \hat{\boldsymbol{\theta}} + \cos \phi \hat{\boldsymbol{\phi}} \right. \\
&\quad \left. + (2 \sin \theta \sin \phi \hat{\mathbf{r}} - \cos \theta \sin \phi \hat{\boldsymbol{\theta}} - \cos \phi \hat{\boldsymbol{\phi}}) \left(\frac{1}{k^2 r^2} - \frac{i}{kr} \right) \right. \\
&\quad \left. - 2 \left(1 + \frac{i}{kr} \right) (\sin \phi \hat{\boldsymbol{\theta}} + \cos \theta \cos \phi \hat{\boldsymbol{\phi}}) \right\} \\
&= -k^2 a^3 E_0 \frac{e^{i(kr-\omega t)}}{2r} \left\{ 2 \sin \theta \sin \phi \left(\frac{1}{k^2 r^2} - \frac{i}{kr} \right) \hat{\mathbf{r}} \right. \\
&\quad \left. + \sin \phi \left[\cos \theta \left(1 - \frac{1}{k^2 r^2} + \frac{i}{kr} \right) - 2 \left(1 + \frac{i}{kr} \right) \right] \hat{\boldsymbol{\theta}} \right. \\
&\quad \left. + \cos \phi \left[1 - \frac{1}{k^2 r^2} + \frac{i}{kr} - 2 \cos \theta \left(1 + \frac{i}{kr} \right) \right] \hat{\boldsymbol{\phi}} \right\}. \tag{17}
\end{aligned}$$

On the surface of the sphere, $r = a$, the scattered electromagnetic fields are, to the leading approximation when $ka \ll 1$,⁵

$$\mathbf{E}_{\text{scat}}(r = a) \approx E_0 e^{-i\omega t} (2 \sin \theta \cos \phi \hat{\mathbf{r}} - \cos \theta \cos \phi \hat{\boldsymbol{\theta}} + \sin \phi \hat{\boldsymbol{\phi}}), \tag{18}$$

$$\mathbf{B}_{\text{scat}}(r = a) \approx -\frac{E_0}{2} e^{-i\omega t} (2 \sin \theta \sin \phi \hat{\mathbf{r}} - \cos \theta \sin \phi \hat{\boldsymbol{\theta}} - \cos \phi \hat{\boldsymbol{\phi}}). \tag{19}$$

In the same approximation, the incident electromagnetic fields at the surface of the sphere are

$$\mathbf{E}_{\text{in}}(r = a) \approx E_0 e^{-i\omega t} \hat{\mathbf{x}} = E_0 e^{-i\omega t} (\sin \theta \cos \phi \hat{\mathbf{r}} + \cos \theta \cos \phi \hat{\boldsymbol{\theta}} - \sin \phi \hat{\boldsymbol{\phi}}), \tag{20}$$

$$\mathbf{B}_{\text{in}}(r = a) \approx E_0 e^{-i\omega t} \hat{\mathbf{y}} = E_0 e^{-i\omega t} (\sin \theta \sin \phi \hat{\mathbf{r}} + \cos \theta \sin \phi \hat{\boldsymbol{\theta}} + \cos \phi \hat{\boldsymbol{\phi}}). \tag{21}$$

Thus, the total electric field,

$$\mathbf{E}_{\text{tot}}(r = a) = \mathbf{E}_{\text{in}}(r = a) + \mathbf{E}_{\text{scat}}(r = a) = 3E_0 e^{-i\omega t} \sin \theta \cos \phi \hat{\mathbf{r}}, \tag{22}$$

on the surface of the sphere is purely radial, and the total magnetic field,

$$\mathbf{B}_{\text{tot}}(r = a) = \mathbf{B}_{\text{in}}(r = a) + \mathbf{B}_{\text{scat}}(r = a) = \frac{3}{2} E_0 e^{-i\omega t} (\cos \theta \sin \phi \hat{\boldsymbol{\theta}} + \cos \phi \hat{\boldsymbol{\phi}}), \tag{23}$$

⁵If the fields were to be used to compute the force and torque on the sphere via the Maxwell stress tensor, terms of order $k^2 a^2$ must be considered. See secs. 2.3.1-2 for a different method.

is purely tangential, as expected for a perfect conductor.⁶

The total charge density σ_{tot} on the surface of the conducting sphere follows from Gauss' law as

$$\sigma_{\text{tot}} = \frac{\mathbf{E}_{\text{tot}}(r = a) \cdot \hat{\mathbf{r}}}{4\pi} = \frac{3E_0}{4\pi} e^{-i\omega t} \sin \theta \cos \phi = \frac{3}{2} \sigma_{\text{scat}}, \quad (24)$$

where σ_{scat} is the surface charge density corresponding to the scattered field (18). Similarly, the total current density \mathbf{K}_{tot} on the surface of the sphere follows from Ampère's law as

$$\mathbf{K}_{\text{tot}} = \frac{c}{4\pi} \hat{\mathbf{r}} \times \mathbf{B}_{\text{tot}}(r = a) = \frac{3cE_0}{8\pi} e^{-i\omega t} (-\cos \phi \hat{\boldsymbol{\theta}} + \cos \theta \sin \phi \hat{\boldsymbol{\phi}}) = 3\mathbf{K}_{\text{scat}}, \quad (25)$$

where \mathbf{K}_{scat} is the surface current density corresponding to the scattered field (19).

We can now discuss the energy flow in the vicinity of the conductor sphere from two perspectives. These two views have the same implications for energy flow in the far zone, but differ in their description of the near zone.

First, we can consider the Poynting vector constructed from the total electromagnetic fields,

$$\mathbf{S}_{\text{tot}} = \frac{c}{4\pi} \mathbf{E}_{\text{tot}} \times \mathbf{B}_{\text{tot}}. \quad (26)$$

Because the tangential component of the total electric field vanishes at the surface of the sphere, lines of the total Poynting vector do not begin or end on the sphere, but rather they pass by it tangentially. In this view, the sphere does not absorb or emit energy, but simply redirects (scatters) the flow of energy from the incident wave.

However, this view does not correspond closely to the “microscopic” interpretation that atoms in the sphere are excited by the incident wave and emit radiation as a result, thereby creating the scattered wave. We obtain a second view of the energy flow that better matches the “microscopic” interpretation if we write

$$\begin{aligned} \mathbf{S}_{\text{tot}} &= \frac{c}{4\pi} \mathbf{E}_{\text{tot}} \times \mathbf{B}_{\text{tot}} \\ &= \frac{c}{4\pi} (\mathbf{E}_{\text{in}} + \mathbf{E}_{\text{scat}}) \times (\mathbf{B}_{\text{in}} + \mathbf{B}_{\text{scat}}) \\ &= \frac{c}{4\pi} \mathbf{E}_{\text{in}} \times \mathbf{B}_{\text{in}} + \frac{c}{4\pi} (\mathbf{E}_{\text{in}} \times \mathbf{B}_{\text{scat}} + \mathbf{E}_{\text{scat}} \times \mathbf{B}_{\text{in}}) + \frac{c}{4\pi} \mathbf{E}_{\text{scat}} \times \mathbf{B}_{\text{scat}} \\ &= \mathbf{S}_{\text{in}} + \mathbf{S}_{\text{interaction}} + \mathbf{S}_{\text{scat}}. \end{aligned} \quad (27)$$

Since the scattered fields (18)-(19) at the surface of the sphere include tangential components for both the electric and the magnetic field, the scattered Poynting vector, \mathbf{S}_{scat} , has a radial component, whose time average we wish to interpret as the flow of energy radiated by the sphere. The scattered Poynting vector at any r is given by

$$\begin{aligned} \langle \mathbf{S}_{\text{scat}} \rangle &= \frac{c}{8\pi} \text{Re}(\mathbf{E}_{\text{scat}}^* \times \mathbf{B}_{\text{scat}}) \\ &= \frac{c}{8\pi} \text{Re} \left[(E_{\theta, \text{scat}}^* B_{\phi, \text{scat}} - E_{\phi, \text{scat}}^* B_{\theta, \text{scat}}) \hat{\mathbf{r}} + (E_{\phi, \text{scat}}^* B_{r, \text{scat}} - E_{r, \text{scat}}^* B_{\phi, \text{scat}}) \hat{\boldsymbol{\theta}} \right] \end{aligned}$$

⁶The surface current density \mathbf{K} on the sphere is given by $\mathbf{K} = (c/4\pi) \hat{\mathbf{r}} \times \mathbf{B}_{\text{tot}}(r = a) = (3E_0 c/8\pi) e^{-i\omega t} (\cos \theta \sin \phi \hat{\boldsymbol{\phi}} - \cos \phi \hat{\boldsymbol{\theta}})$. This is nonzero on the “equator,” $\theta = 90^\circ$, so current flows between the two “sides” of the sphere, in contrast to the case of a thin metallic screen [11], which partly explains why scattering is stronger from a small sphere than from a small disk (footnote 4).

$$\begin{aligned}
& + (E_{r,\text{scat}}^* B_{\theta,\text{scat}} - E_{\theta,\text{scat}}^* B_{r,\text{scat}}) \hat{\phi} \\
= & \frac{c}{8\pi} \frac{k^4 a^6 E_0^2}{r^2} \left\{ \left[\cos^2 \phi \left(\frac{1}{2} - \cos \theta \right)^2 + \sin^2 \phi \left(1 - \frac{\cos \theta}{2} \right)^2 \right] \hat{\mathbf{r}} \right. \\
& \left. - \frac{1}{k^4 r^4} \left(\frac{\cos \theta}{2} \hat{\mathbf{r}} + \sin \theta \hat{\boldsymbol{\theta}} \right) \right\}. \tag{28}
\end{aligned}$$

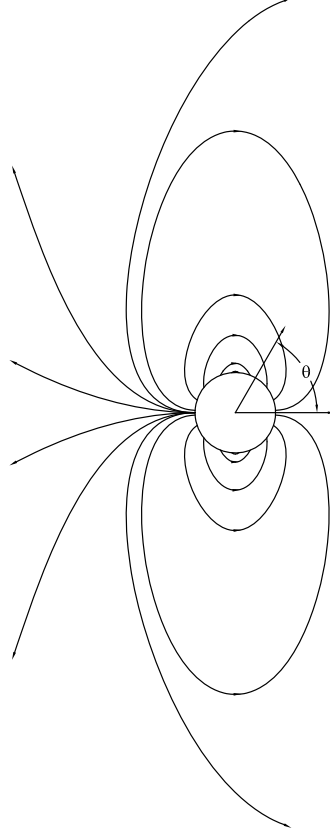
The radial term of eq. (28) in square brackets is identical to the far-zone Poynting vector, while the other radial term is antisymmetric in $\cos \theta$. Hence, the time-average flow of scattered energy across any sphere of radius $r > a$ corresponds to power

$$\langle P_{\text{scat}} \rangle = r^2 \int \langle \mathbf{S}_{\text{scat}} \rangle \cdot \hat{\mathbf{r}} d\Omega = \frac{c E_0^2}{8\pi} \frac{10\pi a^2}{3} k^4 a^4 = \langle P_{\text{rad}} \rangle. \tag{29}$$

However, close to the sphere we find additional terms in $\langle \mathbf{S}_{\text{scat}} \rangle$, so that in the near zone $\langle \mathbf{S}_{\text{rad}} \rangle \neq \langle \mathbf{S}_{\text{scat}} \rangle$. Indeed, at the surface of the sphere we find

$$\begin{aligned}
\langle \mathbf{S}_{\text{scat}}(r = a) \rangle & = \frac{c}{8\pi} E_0^2 \left\{ k^4 a^4 \left[\cos^2 \phi \left(\frac{1}{2} - \cos \theta \right)^2 + \sin^2 \phi \left(1 - \frac{\cos \theta}{2} \right)^2 \right] \hat{\mathbf{r}} \right. \\
& \quad \left. - \left(\frac{\cos \theta}{2} \hat{\mathbf{r}} + \sin \theta \hat{\boldsymbol{\theta}} \right) \right\} \\
& \approx -\frac{c}{8\pi} E_0^2 \left(\frac{\cos \theta}{2} \hat{\mathbf{r}} + \sin \theta \hat{\boldsymbol{\theta}} \right) = -\frac{c}{8\pi} E_0^2 \left(\frac{\hat{\mathbf{z}}}{2} + \frac{3 \sin \theta}{2} \hat{\boldsymbol{\theta}} \right) \tag{30}
\end{aligned}$$

The leading radial term of the scattered Poynting vector at the surface of the sphere corresponds to a large energy being emitted by the hemisphere facing the incident wave, and an equal amount of energy being absorbed by the opposite hemisphere. The energy radiated into the far zone is negligible compared to the leading terms when $ka \ll 1$. As a consequence, the relatively few lines of $\langle \mathbf{S}_{\text{scat}} \rangle$ that do not curl back onto the sphere emanates from very close to the pole of the sphere facing the incident wave, as sketched in the figure below.



This extreme localization of the origin of the lines of the far-field Poynting vector to one pole of the sphere suggests that there is limited merit in associating lines of the time-average scattered Poynting vector with the source of radiation on the sphere.

Of course, the conducting sphere is not an energy source by itself, and the radiated energy is equal to the energy absorbed from the incident wave. For a description of the flow of energy that is absorbed, we look to the time-average of the incident and interaction terms of eq. (27). However, lines of the incident Poynting vector,

$$\langle \mathbf{S}_{\text{in}} \rangle = \frac{c}{8\pi} E_0^2 \hat{\mathbf{z}} = \frac{c}{8\pi} E_0^2 (\cos \theta \hat{\mathbf{r}} - \sin \theta \hat{\boldsymbol{\theta}}), \quad (31)$$

enter and leave the sphere with equal strength, and are therefore not to be associated with energy transfer to the radiation fields. So, we look to the interaction term,

$$\begin{aligned} \langle \mathbf{S}_{\text{interaction}} \rangle &= \frac{c}{8\pi} \text{Re} \left[(E_{\theta, \text{scat}}^* B_{\phi, \text{in}} + E_{\theta, \text{in}}^* B_{\phi, \text{scat}} - E_{\phi, \text{scat}}^* B_{\theta, \text{in}} - E_{\phi, \text{in}}^* B_{\theta, \text{scat}}) \hat{\mathbf{r}} \right. \\ &\quad \left. + (E_{\phi, \text{scat}}^* B_{r, \text{in}} + E_{\phi, \text{in}}^* B_{r, \text{scat}} - E_{r, \text{scat}}^* B_{\phi, \text{in}} - E_{r, \text{in}}^* B_{\phi, \text{scat}}) \hat{\boldsymbol{\theta}} \right. \\ &\quad \left. + (E_{r, \text{scat}}^* B_{\theta, \text{in}} + E_{r, \text{in}}^* B_{\theta, \text{scat}} - E_{\theta, \text{scat}}^* B_{r, \text{in}} - E_{\theta, \text{in}}^* B_{r, \text{scat}}) \hat{\boldsymbol{\phi}} \right] \\ &= \frac{c}{8\pi} \frac{k^2 a^3 E_0^2}{r} \left\{ \left[-\cos[kr(1 - \cos \theta)] \frac{\cos \theta}{2k^2 r^2} \right. \right. \\ &\quad \left. \left. - (1 + \cos \theta) \left[\cos^2 \phi \left(\cos \theta - \frac{1}{2} \right) + \sin^2 \phi \left(1 - \frac{\cos \theta}{2} \right) \right] \times \right. \right. \\ &\quad \left. \left. \left(\frac{\sin[kr(1 - \cos \theta)]}{kr} - \cos[kr(1 - \cos \theta)] \right) \right] \hat{\mathbf{r}} \right\} \end{aligned}$$

$$\begin{aligned}
& + \left[\cos[kr(1 - \cos \theta)] \frac{\sin \theta}{k^2 r^2} \left(2 - \frac{9}{2} \cos^2 \phi \right) + \dots \right] \hat{\boldsymbol{\theta}} \\
& + \left[\frac{9}{8} \cos[kr(1 - \cos \theta)] \frac{\sin 2\theta \sin 2\phi}{k^2 r^2} + \dots \right] \hat{\boldsymbol{\phi}} \Big\}, \tag{32}
\end{aligned}$$

where the omitted terms are small close to the sphere. Note that in the far zone the time-average interaction Poynting vector contains terms that vary as $1/r$ times $\cos[kr(1 - \cos \theta)]$. These large terms oscillate with radius r with period λ , and might be said to describe a radial “sloshing” of energy in the far zone, rather than a radial flow. It appears in practice that one cannot detect this “sloshing” by means of a small antenna placed in the far zone, so we consider these terms to be unphysical. Nonetheless, it is interesting that they appear in the formalism.

At the surface of the sphere we have, again for $ka \ll 1$,

$$\langle \mathbf{S}_{\text{interaction}}(r = a) \rangle \approx \frac{c}{8\pi} E_0^2 \left[-\frac{\cos \theta}{2} \hat{\mathbf{r}} + \sin \theta \left(2 - \frac{9}{2} \cos^2 \phi \right) \hat{\boldsymbol{\theta}} + \frac{9}{8} \sin 2\theta \sin 2\phi \hat{\boldsymbol{\phi}} \right]. \tag{33}$$

The total Poynting vector on the surface of the sphere is the sum of eqs. (30), (31) and (33),

$$\langle \mathbf{S}_{\text{tot}}(r = a) \rangle \approx \frac{c}{8\pi} E_0^2 \left(-\frac{9}{2} \sin \theta \cos^2 \phi \hat{\boldsymbol{\theta}} + \frac{9}{8} \sin 2\theta \sin 2\phi \hat{\boldsymbol{\phi}} \right). \tag{34}$$

The radial component of the total time-average Poynting vector vanishes on the surface of the sphere, in the leading approximation, as expected for a perfect conductor.

However, the leading approximation fails to account for the small net outward flow of energy (29) from the surface of the sphere. Therefore, we examine a higher approximation to the radial component of the time-average interaction Poynting vector,

$$\begin{aligned}
\langle \mathbf{S}_{\text{interaction}}(r = a) \rangle \cdot \hat{\mathbf{r}} \approx & \frac{c}{8\pi} E_0^2 \left\{ -\frac{\cos \theta}{2} + k^2 a^2 \frac{\cos \theta}{4} (1 - \cos \theta)^2 - k^4 a^4 \frac{\cos \theta}{48} (1 - \cos \theta)^4 \right. \\
& + k^2 a^2 (1 + \cos \theta) \left[\cos^2 \phi \left(\cos \theta - \frac{1}{2} \right) + \sin^2 \phi \left(1 - \frac{\cos \theta}{2} \right) \right] \times \\
& \left. \left[\cos \theta - \frac{k^2 a^2}{6} (2 - 3 \cos \theta + \cos^3 \theta) \right] \right\}. \tag{35}
\end{aligned}$$

If in addition we now average over ϕ , the expression in brackets in the middle line of eq. (35) reduces to $(1 + \cos \theta)/4$, and our new average is

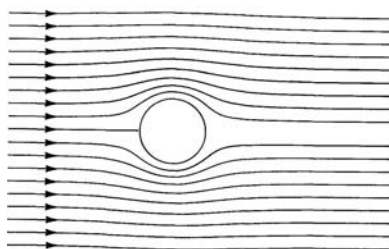
$$\begin{aligned}
\langle \mathbf{S}_{\text{interaction}}(r = a) \rangle \cdot \hat{\mathbf{r}} \approx & \frac{c}{8\pi} E_0^2 \left\{ -\frac{\cos \theta}{2} + k^2 a^2 \frac{\cos \theta}{2} (1 + \cos^2 \theta) - k^4 a^4 \frac{\cos \theta}{48} (1 - \cos \theta)^4 \right. \\
& \left. - \frac{k^4 a^4}{24} (1 + \cos \theta)^2 (2 - 3 \cos \theta + \cos^3 \theta) \right\} \\
= & \frac{c}{8\pi} E_0^2 \left\{ -\frac{\cos \theta}{2} + k^2 a^2 \frac{\cos \theta}{2} (1 + \cos^2 \theta) \right. \tag{36} \\
& \left. - \frac{k^4 a^4}{48} (5 - 2 \cos \theta - 2 \cos^2 \theta - 8 \cos^3 \theta + 5 \cos^4 \theta + 2 \cos^5 \theta) \right\}.
\end{aligned}$$

Integrating this over the surface of the sphere, we find the time-average power absorbed by the sphere due to the interaction fields to be

$$\langle P_{\text{interaction}} \rangle = a^2 \int \langle \mathbf{S}_{\text{interaction}} \rangle \cdot \hat{\mathbf{r}} \, d\Omega = -\frac{cE_0^2}{8\pi} \frac{4\pi a^2}{9} k^4 a^4 \neq -\langle P_{\text{scat}} \rangle. \quad (37)$$

I am disappointed that we have not achieved a complete accounting of energy flow at the surface of the sphere. However, we recall that the metallic boundary condition that $\mathbf{E}_{\parallel} = 0$ on the surface of the sphere is only satisfied in the limit that $ka \rightarrow 0$ in our analysis. In this limit we, of course, recover conservation of energy in the rather trivial form that no energy is absorbed or radiated by the sphere.

A similar exercise was made by Bohren [12] who made a numerical calculation of $\langle \mathbf{S}_{\text{in}} \rangle + \langle \mathbf{S}_{\text{interaction}} \rangle$ for a small aluminum sphere, with results as shown below.



This complements the figure on p. 7 in that the nonscattered Poynting flux touches the sphere only at its pole facing the incident flux, from which point all the scattered Poynting flux appears to emanate.

This exercise permits an additional perspective on analysis of radiation from antennas. Suppose that instead of knowing that a plane wave was incident on the conducting sphere, we were simply given the surface current distribution \mathbf{K}_{scat} of eq. (25). Then, by use of retarded potentials, or the “antenna formula” (*e.g.*, eq. (14.70) of [5]), we could calculate the radiated power in the far zone, and would arrive at the usual expression (28) (ignoring the terms that fall off as $1/r^6$). However, this procedure would lead to an incomplete understanding of the near zone in that additional charges, currents and fields are required to satisfy the metallic boundary conditions at the surface of the conductors of the antenna.

In the present example, the excitation of the conducting sphere by an external plane wave leads to a total surface current that is three times larger than the current \mathbf{K}_{scat} . For a good, but not perfectly conducting sphere, an analysis based on \mathbf{K}_{scat} alone would lead to only 1/9 the actual amount of Joule heating of the sphere. And, if we attempted to assign some kind of impedance or radiation resistance to the sphere via the form $P_{\text{rad}} = R_{\text{rad}} I_0^2/2$, where I_0 is meant to be a measure of the peak total current, an analysis based only on knowledge the current \mathbf{K}_{scat} would lead to a value of R_{rad} that is 9 times larger than a value based on the total current.

2.3 Scattering of a Circularly Polarized Wave

If the incident wave is circularly polarized the incident fields can be written as

$$\mathbf{E}_{\text{in}} = \mathbf{E}_0 e^{i(kz - \omega t)}, \quad \mathbf{B}_{\text{in}} = \mathbf{B}_0 e^{i(kz - \omega t)}, \quad (38)$$

where

$$\mathbf{E}_0 = E_0 \frac{\hat{\mathbf{x}} \pm i\hat{\mathbf{y}}}{\sqrt{2}}, \quad \mathbf{B}_0 = \hat{\mathbf{z}} \times \mathbf{E}_0 = \mp i\mathbf{E}_0. \quad (39)$$

The dipole moments induced on the conducting sphere by the incident wave are again given by eqs. (3)-(4), and the scattered electric field in the far zone follows from eq. (4) as

$$\begin{aligned} \mathbf{E}_{\text{scat}} &= -k^2 a^3 E_0 \frac{e^{i(kr-\omega t)}}{\sqrt{2}r} \left(\hat{\mathbf{n}} \times [(\hat{\mathbf{x}} \pm i\hat{\mathbf{y}}) \times \hat{\mathbf{n}}] + \frac{1}{2} \hat{\mathbf{n}} \times [\hat{\mathbf{z}} \times (\hat{\mathbf{x}} \pm i\hat{\mathbf{y}})] \right) \\ &= -k^2 a^3 E_0 \frac{e^{i(kr-\omega t)}}{\sqrt{2}r} \left[(\hat{\mathbf{x}} \pm i\hat{\mathbf{y}}) \left(1 - \frac{(\hat{\mathbf{n}} \cdot \hat{\mathbf{z}})}{2} \right) - \left(\hat{\mathbf{n}} - \frac{\hat{\mathbf{z}}}{2} \right) [\hat{\mathbf{n}} \cdot (\hat{\mathbf{x}} \pm i\hat{\mathbf{y}})] \right]. \end{aligned} \quad (40)$$

Inserting this in (1) we find

$$\frac{d\sigma}{d\Omega} = k^4 a^6 \left[\left(1 - \frac{\hat{\mathbf{n}} \cdot \hat{\mathbf{z}}}{2} \right)^2 - \frac{3}{8} [(\hat{\mathbf{n}} \cdot \hat{\mathbf{x}})^2 + (\hat{\mathbf{n}} \cdot \hat{\mathbf{y}})^2] \right]. \quad (41)$$

It suffices to consider an observer in the x - z plane, for which $\hat{\mathbf{n}} \cdot \hat{\mathbf{x}} = \sin \theta$, $\hat{\mathbf{n}} \cdot \hat{\mathbf{y}} = 0$, $\hat{\mathbf{n}} \cdot \hat{\mathbf{z}} = \cos \theta$. Then, eq. (41) yields

$$\frac{d\sigma}{d\Omega} = k^4 a^6 \left[\frac{5}{8} (1 + \cos^2 \theta) - \cos \theta \right], \quad \sigma = \int \frac{d\sigma}{d\Omega} d\Omega = \frac{10\pi a^2}{3} k^4 a^4. \quad (42)$$

as found in eqs. (9)-(10) for an unpolarized incident wave.⁷

2.3.1 Force on the Sphere

The electric field must be perpendicular to the surface of a perfect conductor (at rest), so the Poynting vector $\mathbf{S} = c\mathbf{E} \times \mathbf{B}/4\pi$ has zero component perpendicular to the surface. That is, a perfect conductor absorbs no energy from the incident wave. However, the conductor can acquire momentum (and angular momentum) as a result of scattering of the wave.⁸ Here, we consider the momentum (and angular momentum) density in the far zone, where it can be related to the energy density, to infer the rate of change of (angular) momentum of the sphere, and hence the force (torque) on the sphere.

The differential cross section (42) peaks at $\theta = 180^\circ$ (backscattering), so more energy is scattered backwards than forwards. For electromagnetic waves in vacuum (far from any conductors) the (time-average) momentum density $\langle \mathbf{p} \rangle$ is related to the (time-average) energy density $\langle u \rangle$ by⁹

$$\langle \mathbf{p} \rangle = \frac{\langle u \rangle}{c} \hat{\mathbf{n}}. \quad (43)$$

⁷The cross section for scattering (at normal incidence) off a perfectly conducting disk of radius a is about 1/6 that of eq. (42) [9, 10]. This suggests that the force and torque on a conducting disk is about 1/6 of that found below for a conducting sphere. See also [14].

⁸While the Poynting vector describes the flux of electromagnetic energy, the fluxes of momentum and angular momentum are described by tensors. See, for example, sec. 3.2 and prob. 3.5 of [13].

⁹The momentum density can also be evaluated as $\langle \mathbf{p}_{\text{scat}} \rangle = \langle \mathbf{S}_{\text{scat}} \rangle / c^2 = \text{Re}(\mathbf{E}_{\text{scat}} \times \mathbf{B}_{\text{scat}}^*) / 8\pi c$, using the fields given in eqs. (51)-(52).

The net flux of scattered momentum (which propagates at speed c) along the z -axis is

$$\begin{aligned} \frac{d\langle P_z \rangle}{dt} &= \int \hat{\mathbf{z}} \cdot c r^2 \langle \mathbf{p} \rangle_{\text{scat}} d\Omega = \int r^2 \langle u \rangle_{\text{scat}} \cos \theta d\Omega = \int \frac{r^2 |\mathbf{E}_{\text{scat}}|^2}{8\pi} \cos \theta d\Omega \\ &= \int \frac{E_0^2}{8\pi} \frac{d\sigma}{d\Omega} \cos \theta d\Omega = \frac{E_0^2 k^4 a^6}{4} \int \left[\frac{5}{8}(1 + \cos^2 \theta) - \cos \theta \right] \cos \theta d\cos \theta = -\frac{E_0^2 k^4 a^6}{6}. \end{aligned} \quad (44)$$

The reaction force on the sphere is the negative of this,

$$F_z = -\frac{d\langle P_z \rangle}{dt} = \frac{E_0^2 k^4 a^6}{6} = \pi a^2 \frac{E_0^2 k^4 a^4}{6\pi} \equiv \pi a^2 P_{\text{rad}}, \quad (45)$$

where $P_{\text{rad}} = E_0^2 k^4 a^4 / 6\pi$ is the effective radiation pressure on the sphere due to the incident wave.

The nominal radiation pressure of the incident plane wave is

$$P_{\text{in}} = c \langle p_{\text{in}} \rangle = \langle u_{\text{in}} \rangle = \frac{E_0^2}{8\pi}, \quad (46)$$

so the effective radiation pressure on the sphere can be written as

$$\langle P_{\text{rad}} \rangle = \frac{4k^4 a^4}{3} P_{\text{in}} \ll P_{\text{in}}. \quad (47)$$

That is, the force on the small conducting sphere due to scattering of the incident electromagnetic wave is much less than if the sphere totally absorbed the momentum of the incident wave.^{10,11,12}

2.3.2 Torque on the Sphere

The circularly polarized incident wave carries angular momentum with density

$$\langle l_{\text{in},z} \rangle = \pm \frac{\langle p_{\text{in},z} \rangle}{k} = \pm \frac{\langle u_{\text{in}} \rangle}{ck} = \pm \frac{E_0^2}{8\pi ck}. \quad (49)$$

The scattered wave carries (time-average) angular momentum density

$$\langle \mathbf{l}_{\text{scat}} \rangle = \frac{\mathbf{r}}{8\pi c} \times \text{Re}(\mathbf{E}_{\text{scat}} \times \mathbf{B}_{\text{scat}}^*) = \frac{r}{8\pi c} \text{Re}[(\hat{\mathbf{r}} \cdot \mathbf{B}_{\text{scat}}^*) \mathbf{E}_{\text{scat}} - (\hat{\mathbf{r}} \cdot \mathbf{E}_{\text{scat}}) \mathbf{B}_{\text{scat}}^*]. \quad (50)$$

¹⁰The force on spheres due to an electromagnetic wave was first calculated (using the Maxwell stress tensor) in [15], although eq. (94) there seems to have a factor 14/3 rather than the 4/3 of eq. (47). See also [16]. However, my computation via the stress tensor over a sphere of large radius r gives, using eq. (51),

$$\begin{aligned} \langle F_z \rangle &= 2\pi r^2 \int d\cos \theta \cos \theta \langle T_{rr} \rangle = -2\pi r^2 \int d\cos \theta \cos \theta \frac{|E_\theta|^2 + |E_\phi|^2}{8\pi} \\ &= -\frac{E_0^2 k^4 a^6}{8} \int d\cos \theta \cos \theta \left(\cos^2 \theta - \cos \theta + \frac{1}{4} + 1 - \cos \theta + \frac{\cos^2 \theta}{4} \right) = \frac{E_0^2 k^4 a^6}{6}, \end{aligned} \quad (48)$$

as found in eq. (45).

¹¹The force of radiation pressure was first measured in [17, 18]. See also [19].

¹²This analysis tacitly assumes that the sphere remains at rest due to an external force F_z , such that the sphere does not take on any kinetic energy. If the sphere is in motion there is transfer of energy via the Poynting vector between the fields and the sphere, as discussed in [20].

To obtain a density that falls off as $1/r^2$ we need the radial terms in the scattered fields that fall off as $1/r^2$ (as well as the transverse field of order $1/r$). We recall eqs. (16)-(17) for the case of x -polarization, and note that the fields for y polarization follow from these via the substitutions $\phi \rightarrow \phi - \pi/2$, $\cos \phi \rightarrow \sin \phi$, and $\sin \phi \rightarrow -\cos \phi$,

$$\begin{aligned} \mathbf{E}_{\text{scat}}(\mathbf{r}, t) \approx & E_0 k^2 a^3 \frac{e^{i(kr-\omega t)}}{\sqrt{2}r} \left\{ -\frac{2i}{kr} \sin \theta (\cos \phi \pm i \sin \phi) \hat{\mathbf{r}} \right. \\ & \left. + (\cos \phi \pm i \sin \phi) \left(\cos \theta - \frac{1}{2} \right) \hat{\boldsymbol{\theta}} - (\sin \phi \mp i \cos \phi) \left(1 - \frac{\cos \theta}{2} \right) \hat{\boldsymbol{\phi}} \right\}, \end{aligned} \quad (51)$$

$$\begin{aligned} \mathbf{B}_{\text{scat}}(\mathbf{r}, t) \approx & E_0 k^2 a^3 \frac{e^{i(kr-\omega t)}}{\sqrt{2}r} \left\{ -\frac{i}{kr} \sin \theta (\sin \phi \mp i \cos \phi) \hat{\mathbf{r}} \right. \\ & \left. + (\sin \phi \mp i \cos \phi) \left(1 - \frac{\cos \theta}{2} \right) \hat{\boldsymbol{\theta}} + (\cos \phi \pm i \sin \phi) \left(\cos \theta - \frac{1}{2} \right) \hat{\boldsymbol{\phi}} \right\}. \end{aligned} \quad (52)$$

Then,

$$\langle \mathbf{l}_{\text{scat}} \rangle = \pm \frac{3E_0^2 k^4 a^6}{32\pi r^2 k c} \sin \theta \hat{\boldsymbol{\theta}}. \quad (53)$$

The net flux of scattered angular momentum (which propagates at speed c) along the z -axis is¹³

$$\frac{d\langle L_z \rangle}{dt} = \int \hat{\mathbf{z}} \cdot c r^2 \langle \mathbf{l}_{\text{scat}} \rangle d\Omega = \mp \frac{3E_0^2 k^4 a^6}{16k} \int \sin^2 \theta d\cos \theta = \mp \frac{E_0^2 k^4 a^6}{4k}. \quad (54)$$

The torque required to keep the sphere at rest is the negative of this,

$$\tau = -\frac{d\langle L_z \rangle}{dt} = \pm \frac{E_0^2 k^4 a^6}{4k} = \pm \pi a^2 \frac{E_0^2 k^4 a^4}{4\pi k}. \quad (55)$$

The angular momentum per unit time incident on the area of the sphere is $\pi a^2 c \langle l_{\text{in},z} \rangle = \pm \pi a^2 E_0^2 / 8\pi k$, so the fraction of the angular momentum incident on the sphere that is transferred to it is only $2k^4 a^4 \ll 1$.¹⁴

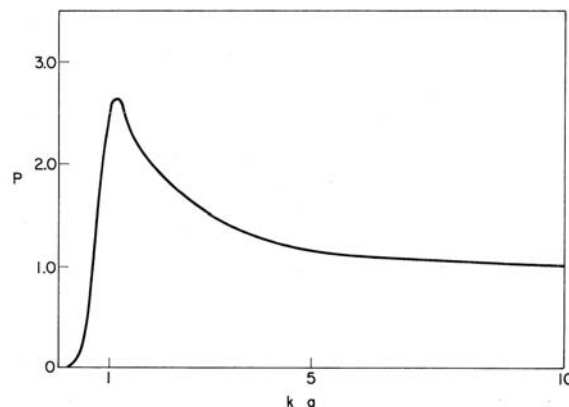
The first mechanical detection of the angular momentum of light was by Beth [21], and one detection of angular momentum of microwaves has been reported [22, 23].

¹³The classical form (53) for angular momentum density indicates that the local angular momentum vector is perpendicular to the (local) direction of propagation of the wave, whereas in the quantum view the angular momentum vector is parallel to the momentum vector (if these are known/measured). In the quantum view the wave(function) as a whole carries angular momentum, which cannot be further localized without a measurement. That is, eq. (53) represents a level of detail not supported in the quantum view. However, a classical expression like eq. (54) that characterizes the angular momentum of the entire wave will agree with the quantum view (of the average over many photons).

¹⁴If it is desired that the sphere experience a larger torque due to the incident circularly polarized wave, the sphere must absorb (or scatter) a significant fraction of that wave. In the present case of a conducting sphere it would be favorable to choose the radius a to be about $\lambda/5$, in which case the scattering cross section exhibits a “resonance” peak, shown in the figure below from [16], as which the cross section is $2.6\pi a^2 \approx \lambda^2/3$.

References

- [1] J.J. Thomson, *Recent Researches in Electricity and Magnetism* (Clarendon Press, 1893), http://physics.princeton.edu/~mcdonald/examples/EM/thomson_recent_researches_in_electricity.pdf
- [2] J.H. Poynting, *On the Transfer of Energy in the Electromagnetic Field*, Phil. Trans. Roy. Soc. London **175**, 343 (1884), http://physics.princeton.edu/~mcdonald/examples/EM/poynting_ptrs1_175_343_84.pdf
- [3] C. Huygens, *Treatise on Light* (1678), English translation by S.P. Thompson (Macmillan, 1912), http://physics.princeton.edu/~mcdonald/examples/optics/huygens_treatise_on_light.pdf
- [4] H. Hertz, *The Forces of Electrical Oscillations Treated According to Maxwell's Theory*, Weidemann's Ann. **36**, 1 (1889); reprinted in chap. 9 of H. Hertz, *Electric Waves* (Dover, New York, 1962). A translation by O. Lodge appeared in Nature **39**, 402 (1889), http://physics.princeton.edu/~mcdonald/examples/EM/hertz_electric_waves.pdf
- [5] J.D. Jackson, *Classical Electrodynamics*, 3rd ed. (Wiley, 1999), http://physics.princeton.edu/~mcdonald/examples/EM/jackson_ce3_99.pdf
- [6] K.T. McDonald, *Radiation in the Near Zone of a Hertzian Dipole* (April 22, 2004), <http://physics.princeton.edu/~mcdonald/examples/nearzone.pdf>
- [7] J.J. Thomson, *Conduction of Electricity in Gases*, 2nd ed. (Cambridge U. Press, 1906), http://physics.princeton.edu/~mcdonald/examples/EM/thomson_conduction_of_electricity_through_gases_sec161-163.pdf
- [8] Lord Rayleigh, *On the Incidence of Aerial and Electric Waves upon Small Obstacles in the form of Ellipsoids or Elliptic Cylinders, and on the Passage of Electric Waves through a circular Aperture in a Conducting Screen*, Phil. Mag. **44**, 28 (1897), http://physics.princeton.edu/~mcdonald/examples/EM/rayleigh_pm_44_28_97.pdf
- [9] C.J. Boukamp, *On the diffraction of electromagnetic waves by small circular disks and holes*, Philips Res. Rep. **5**, 401 (1950), http://physics.princeton.edu/~mcdonald/examples/EM/bouwkamp_physica_16_1_50.pdf



A similar effect for a dielectric sphere is discussed in [12]. For linear dipole antennas, the “resonance” condition is that the half-height h be close to $\lambda/4$, as understood by Hertz (chap. 8 of [4]).

- [10] W.H. Eggimann, *Higher Order Evaluation of Electromagnetic Diffraction by Circular Disks*, I.R.E. Trans. Micro. Theor. Tech. **9**, 408 (1961),
http://physics.princeton.edu/~mcdonald/examples/EM/eggimann_iremtt_9_408_61.pdf
- [11] Z.M. Tan and K.T. McDonald, *Symmetries of Electromagnetic Fields Associated with a Plane Conducting Screen* (Jan. 14, 2012),
<http://physics.princeton.edu/~mcdonald/examples/emsymmetry.pdf>
- [12] C.F. Bohren, *How can a particle absorb more than the light incident on it?*, Am. J. Phys. **51**, 323 (2004), http://physics.princeton.edu/~mcdonald/examples/EM/bohren_ajp_51_323_83.pdf
- [13] J. Schwinger, L.L. DeRaad, Jr, K.A. Milton and W.-Y. Tsai, *Classical Electrodynamics* (Perseus Book, 1998), http://physics.princeton.edu/~mcdonald/examples/EM/schwinger_em_98.pdf
- [14] G. Toraldo di Francia, *On a Macroscopic Measurement of the Spin of Electromagnetic Radiation*, Nuovo Cim. **6**, 150 (1957),
http://physics.princeton.edu/~mcdonald/examples/EM/toraldodifracia_nc_6_150_57.pdf
- [15] P. Debye, *Der Lichtdruck auf Kugeln von beliebigem Material*, Ann. d. Phys. **30**, 57 (1909), http://physics.princeton.edu/~mcdonald/examples/EM/debye_ap_30_57_09.pdf
- [16] R. Burn and O. Buneman, *Radiation Pressure on a Conducting Sphere*, SUIPR-112 (1966), http://physics.princeton.edu/~mcdonald/examples/EM/burn_suipr112_66.pdf
- [17] P. Lebedew, *Untersuchungen über die Druckkräfte des Lichtes*, Ann. d. Phys. **6**, 433 (1901), http://physics.princeton.edu/~mcdonald/examples/EM/lebedew_ap_6_433_01.pdf
- [18] E.E. Nichols and G.F. Hull, *The Pressure Due to Radiation*, Phys. Rev. **17**, 26, 91 (1903), http://physics.princeton.edu/~mcdonald/examples/EM/nichols_pr_17_26_03.pdf
- [19] D. Demir, *A table-top demonstration of radiation pressure*, Diplomarbeit, U. Wien (2011), http://physics.princeton.edu/~mcdonald/examples/EM/demir_thesis_11.pdf
- [20] R.C. Restrick, III, *Electromagnetic Scattering by a Moving Conducting Sphere*, Radio Sci. **3**, 1144 (1968), http://physics.princeton.edu/~mcdonald/examples/EM/restrick_rs_3_1144_68.pdf
- [21] R.A. Beth, *Mechanical Detection and Measurement of the Angular Momentum of Light*, Phys. Rev. **50**, 115 (1936),
http://physics.princeton.edu/~mcdonald/examples/optics/beth_pr_50_115_36.pdf
- [22] N. Carrara, *Coppia e momento angolare della radiazione*, Nuovo Cim. **6**, 50 (1949),
http://physics.princeton.edu/~mcdonald/examples/EM/carrara_nc_6_50_49.pdf
- [23] N. Carrara, *Torque and Angular Momentum of Centimetre Electromagnetic Waves*, Nature **164**, 882 (1949),
http://physics.princeton.edu/~mcdonald/examples/EM/carrara_nature_164_882_49.pdf